



Novel composites of *Pennisetum glaucum* with CNT: preparation, characterization and application for the removal of safranin O and methylene blue dyes from single and binary systems

Sarita Yadav¹ · Aruna Yadav¹ · Nisha Bagotia¹ · Ashok K. Sharma² · Surender Kumar¹

Received: 15 September 2021 / Revised: 13 December 2021 / Accepted: 14 December 2021 / Published online: 21 January 2022
© The Author(s), under exclusive licence to Springer-Verlag GmbH Germany, part of Springer Nature 2022

Abstract

Agricultural waste-based adsorbents offer an innovative, cost-effective, and environmentally benign approach for the removal of various dyes from wastewater. Herein, *Pennisetum glaucum*-based novel composites with functionalized carbon nanotubes (CNT) were developed for the effective and efficient removal of methylene blue (MB) and safranin O (SO) dyes from the single and binary systems for the first time. Characterization of as-synthesized composites was performed using various techniques such as field emission scanning electron microscopy (FESEM), Fourier transform infrared spectroscopy (FTIR), X-ray diffraction (XRD), and differential scanning calorimetry (DSC). In batch studies, both the dyes were effectively removed at neutral pH with 0.01 g/10 mL of adsorbent dosage and 10 min of contact time at 30 °C. The adsorption isotherm and kinetic data were well fitted by the Langmuir isotherm and pseudo-second-order model, respectively. The maximum adsorption capacity of the composite containing 0.5% of CNT was 181.81 and 386.1 mgg⁻¹ for MB and SO dyes, respectively, which were 267.29% and 94.61% greater than raw *P. glaucum* adsorbent. The adsorption was spontaneous, exothermic, and physisorption in nature, involving electrostatic, π - π , and H-bonding interactions. The as-prepared adsorbents exhibited excellent reusability, and their adsorption efficiency was maintained even after ten cycles. Finally, the present work suggests a promising strategy for the preparation and application of novel green adsorbents for wastewater remediation.

Keywords Adsorption · Methylene blue · Safranin O · Pearl millet · Carbon nanotubes

1 Introduction

Currently, environmental contamination with dyes occurs on a global scale as a result of an inexorable rise of population and industrialization. More often, different industries use water bodies as sinks to dump their chemical waste. As per the list of top ten polluting industries registered by an international non-profit organization, Pure Earth (2016), dye industries are among the most notable contributing sectors

[1]. It is predicted that nearly 1.6 million tons of 100,000 new synthetic dyes are generated annually for industrial requirements and approximately 10–15% of the unused dye-stuff of this volume is discharged in water bodies directly [2, 3]. However, the complex structure, xenobiotic and non-biodegradable properties, makes them resistant to heat and light, thereby making their removal from wastewater very challenging [4]. Due to this inappropriate handling of these dyes, there are serious pollution risks on the ecosystem such as eutrophication of water bodies and death of plants and animals [5–7]. Safranin O (SO) is a synthetic azine dye and has been used as a food dye in cookies and candies besides being utilized in the dyeing leather, wool, paper, silk, jute fibers, and cotton. Acute exposure to it resulted in detrimental health effects like throat and oral irritation, vomiting and diarrhea, stomach aches, and eye and dermal irritation [8]. Methylene blue (MB) is a cationic dye that is extensively used in the dyeing industry. It is toxic and exerts detrimental several health risks in humans upon exposure such as vomiting, nausea, eye injury and methemoglobinemia [9]. So far,

✉ Ashok K. Sharma
ashoksharma2k18@gmail.com

✉ Surender Kumar
skaushik@cblu.ac.in

¹ Department of Chemistry, Chaudhary Bansi Lal University, Bhiwani, Haryana, India 127021

² Department of Chemistry, Deenbandhu Chhotu Ram University of Science and Technology, Murthal, Sonapat, Haryana, India 131039

decontamination techniques have been employed to remove the dyes from wastewater like ultrafiltration [10], coagulation-flocculation [11, 12], advanced oxidation processes [13], photocatalysis [14], biological treatment [15], chemical reduction [16], and adsorption [17], reverse osmosis [18]. However, adsorption by using low-cost adsorbents is considered as one of the most promising technologies to remediate dye-containing wastewater due to its cost-effectiveness, simplicity of design, availability, easy operation and maintenance, rapidness, high efficiency, and no secondary pollution [19–22], S. [3, 12, 23–25]. The adsorbents which are employed for the adsorption should possess the following features like large specific surface area, physicochemical stability, abundant adsorption sites, non-toxicity, high maximal saturation capacity, and eco-friendly to the environment [26, 27]. The biomass waste-based adsorbents contain oxygenated functional groups like alcohol, ketone, and carboxylic groups, which are responsible for the sequestration of dyes by different adsorption mechanisms. Several agriculture waste materials like rice husk, coffee, peanut husk, activated rice husk [28], sawdust, orange peel, banana pith, and wheat shells have been utilized as adsorbents for the treatment of wastewater [22, 29, 30]. However, the direct use of these adsorbents is not much efficient due to its lower adsorption efficiency and the leaching of soluble organic molecules from adsorbents increases the total organic carbon, biological, and chemical oxygen demand of water [31]. Therefore, different modifications of biomass have been reported in the last few decades to enhance the adsorption capacity.

Pennisetum glaucum belongs to the Poaceae family and Cenchrus genus, commonly known as pearl millet or bajra. India is the major producer of pearl millet both in terms of area (7.47 million ha) and production (9.80 million tons), with average productivity of 1305 kg ha⁻¹ [32]. Its seeds are used as cereals, while other part like leaves and stem remains in the fields as waste and burnt which causes air pollution. Although some researchers have reported the use of the pearl millet husk as an adsorbent in raw form or by using its activated carbon for the removal of dyes and heavy metals [33–38], yet, the composite of pearl millet stem for the removal of dyes is not reported until date to the best of our knowledge.

Carbon nanotubes (CNTs) are typically cylindrical forms of graphene sheets having high porosity, specific surface area, and hollow structures with highly hydrophobic surfaces [39]. These have exceptional properties like ultra-low weight, thermal and chemical stability, and high mechanical strength (A. [23, 40]. The morphology, active sites, and defects of CNTs are responsible for the adsorption of dyes [39]. Furthermore, chemically functionalized CNT surfaces, grafted with specific functional groups like hydroxyl, fluorine, carboxyl, and amine, generate high-affinity sorption sites for increased binding of target adsorbates like dyes via

π - π electron bonding or electrostatic attractions [41–43]. Despite these merits, the practical application of CNTs remains limited by their poor solubility and rapid aggregation in their pristine state [44, 24]. Thus, different CNT composites like CNT-graphene composite, starch-functionalized multi-walled CNTs (MWCNT)/iron oxide composite, Guar gum grafted Fe₃O₄/MWCNTs ternary composite, and CNT-activated carbon fabric composite were used to remove the dyes from wastewater with good adsorption capacity [45]. However, the high cost and use of chemicals in many of these reports have made it necessary to consider other environmentally benign and low-cost supports for CNT for the formation of composites. Also, the existing literature lacks in-depth exploration of the adsorptive potential of composites of CNT with biomass.

In view of the aforesaid, this study involves the use of low-cost, pearl millet stem waste for the fabrication of composites with functionalized CNT for the efficient removal of basic dyes, i.e., MB and SO, for the first time to the best of our knowledge. The overall objective of this report was to develop a simple method to synthesize CNT-biomass composite and its characterization to deliver a more practical and flexible solution for the removal of basic dyes from wastewater which will directly benefit the environment and human health. Furthermore, the effect of different adsorption parameters like temperature, adsorbent dose, time, adsorbate concentration, and pH, on the adsorption efficiency of adsorbents, was studied. Different kinetic models and isotherms were fitted to the experimental data to evaluate the nature of adsorption and the type of interactions for the adsorption of MB and SO dyes on the composite surface. Desorption studies were also carried out to check the renewal efficiency of prepared adsorbents.

2 Materials and methods

2.1 Chemicals and materials

Pennisetum glaucum (pearl millet stem) was collected from the Bhiwani region of Haryana, India, and its identity was confirmed by the National Institute of Science Communications and Information Resources, India. Multi-walled CNTs were purchased from Nanocyl S.A. (Belgium) of NC 7000 industrial grade having carbon purity of 90%, diameter ~ 9.6 nm, length ~ 1.5 μ m, and surface area 250–300 m²g⁻¹. All the used reagents like MB, SO, acetone, HCl, NaOH, deionized water (DI), HNO₃, and H₂SO₄ were purchased of analytical grade from the SRL company and used as received. The stock solutions of dyes were prepared by dissolving 1 g of dye in 1 L of water. Solutions of different concentrations were prepared by diluting the stock solutions with distilled water.

2.2 Preparation of adsorbents

The collected pearl millet raw material (RM) was washed to remove impurities; after that, it was chopped into small pieces and sun-dried to remove the moisture. The dried material was ground and sieved with mesh sizes 60, 80, and 120 BSS, and for further size reduction, it was ball milled for 5–6 h to study the effect of particle size on the removal of dyes. The powdered adsorbent was preserved in an airtight container for further use.

The functionalization of MWCNT with carboxyl groups was done by using the earlier reported method [46]. One gram of MWCNT was added in a 500-mL conical flask containing a 100-mL mixture of H_2SO_4 and HNO_3 (3:1), and the suspension was kept for 1 day. For the fine dispersion of MWCNTs, the solution was ultrasonicated for 4–5 h. After that, the functionalized MWCNTs were filtered by using Whatman filter paper. Several washings with DI water were given to attain the neutral pH of the filtrate. The obtained functionalized CNT was oven-dried and stored for further use.

Three different composites containing different amounts of functionalized CNT were prepared as shown in Fig. 1, by adding 5 g of biomass in different conical flasks containing a solution of 0.025 g, 0.05 g, and 0.102 g of functionalized CNT and 100 mL of DI water. After that, the suspension was ultrasonicated for 2 h for even dispersion of fine particles of CNT. The prepared composites were washed and oven-dried and preserved in an airtight container for further uses. The synthesized composites containing 0.5%, 1%, and 2% CNT and biomass (B) were labelled as 0.5% CNTB, 1% CNTB, and 2% CNTB, respectively.

2.3 Characterization

Different characterization techniques like FESEM (field emission scanning electron microscopy), FTIR (Fourier transform infrared spectroscopy), XRD (X-ray diffraction), and DSC (differential scanning calorimetry) were employed for the analysis of RM and its composites. FESEM images of adsorbents were recorded using a 7610F Plus, JEOL model operated at 5 kV. FTIR analysis of adsorbents was performed using Frontier, Perkin Elmer model where the spectra were recorded in the wavenumber range from 4000 to 500 cm^{-1} . A diffractometer, Rigaku (model MiniFlex-600) was employed to perform the XRD analysis of adsorbents. Furthermore, temperature decomposition and enthalpy changes corresponding to changes in chemical and physical properties of adsorbent were analyzed by using TA Instrument (DSCQ-10 model).

2.4 Batch adsorption experiments

The adsorption capacity and mechanisms were determined by analyzing the kinetic experiments, the effect of solution pH, thermodynamic parameters, and adsorption isotherms by taking a fixed amount of adsorbent in 10-mL aqueous solution of each cationic dye having definite initial dye concentrations in a conical flask (100 mL) and shaking for a certain time on a temperature-controlled magnetic stirrer at preset rpm. The different adsorption analysis parameters like pH (2–12), composites dose (0.005–0.05 g in 10-mL dye aqueous solution), contact time (3–120 min), dye initial concentration (15–60 mg L^{-1}), particle size (250–22.698 μm), and temperature (30–60 $^\circ\text{C}$) were optimized. The pH of the dye solution was controlled by adding 0.1 N HCl and NaOH. The effects of individual parameters were investigated of varying only one parameter while others were fixed. The

Fig. 1 Preparation of composites of raw *P. glaucum*



isoelectric point of the adsorbents was determined using the pH drift method [47]. The kinetic study was performed by taking 0.01 g adsorbent mass in 10 mL of dye solution of concentration 30 mg L⁻¹ at 30 °C for the time intervals of (3, 5, 10, 15, 20, 30, 60 min) at neutral pH. The mathematical expressions of different kinetic models like pseudo-first-order, pseudo-second-order, intraparticle diffusion, and Elovich are given in Eqs. (1–4).

Pseudo-first-order model [48]:

$$\ln(q_e - q_t) = \ln q_e - k_1 t \quad (1)$$

Pseudo-second-order kinetic model [48]:

$$\frac{t}{q_t} = \frac{1}{k_2 q_e^2} + \frac{t}{q_e} \quad (2)$$

Intraparticle diffusion model [48]:

$$q_t = k_i t^{0.5} + c \quad (3)$$

Elovich model [48]:

$$q_t = \frac{1}{\beta} \ln t + \frac{1}{\beta} \ln(\alpha\beta) \quad (4)$$

Here, k_1 (min⁻¹), k_2 (g mg⁻¹ min⁻¹), and k_i (mg g⁻¹ min^{-1/2}) are the rate constants of pseudo-first-order, pseudo-second-order, and intraparticle diffusion kinetic models. c (mg g⁻¹) is the degree of adsorption, t (min) represents time, and α (mg g⁻¹ min⁻¹) denotes the primary rate of adsorption. β denotes the desorption parameter, and it is utilized for the characterization of the degree of chemisorption and activation energy.

The study of different adsorption isotherm experiments was carried out by taking 0.01 g of adsorbent doses in 10 mL of dye solution of different concentrations (15–60 mg L⁻¹) at neutral pH and room temperature. The thermodynamics study was conducted in the temperature range of 30–60 °C (dye concentration 30 mg L⁻¹, adsorbent dosage 0.01 g in 10 mL of dye aqueous solution, pH 7, contact time 10 min). The residual concentration of MB and SO dyes were determined by measuring absorbance at 665 nm and 520 nm, respectively, by using Systronics UV–visible spectrophotometer model 117. The % removal and the quantity of dyes adsorbed onto the unit mass of adsorbents were determined by using the following Eqs. (5–7) [48].

$$R(\%) = \frac{(C_0 - C_e)}{C_0} \times 100 \quad (5)$$

$$q_e = \frac{(C_0 - C_e) \times V}{M} \quad (6)$$

$$q_t = \frac{(C_0 - C_t) \times V}{M} \quad (7)$$

where q_e (mg g⁻¹) is the adsorption capacity of dyes at equilibrium, q_t (mg g⁻¹) is the adsorption capacity of dyes at time t , C_0 (mg L⁻¹) and C_e (mg L⁻¹) are the initial and equilibrium concentrations of dyes, V (L) is the volume of dyes solution, and M (g) is the mass of adsorbents.

Batch adsorption experiments in MB/SO mixed dye solution

To investigate the % dye removal by synthesized adsorbents in the binary mixture of MB and SO dyes, the experiment was carried out by adding 0.01 g of different adsorbents in a conical flask containing 10 mL (5 mL SO + 5 mL MB) solution of dye mixture having an initial concentration of 30 mg L⁻¹; the solution was stirred for 10 min at neutral pH and 30 °C temperature. After that, the final concentration of dye solution was measured with the help of a UV–visible spectrophotometer.

2.5 Regeneration studies

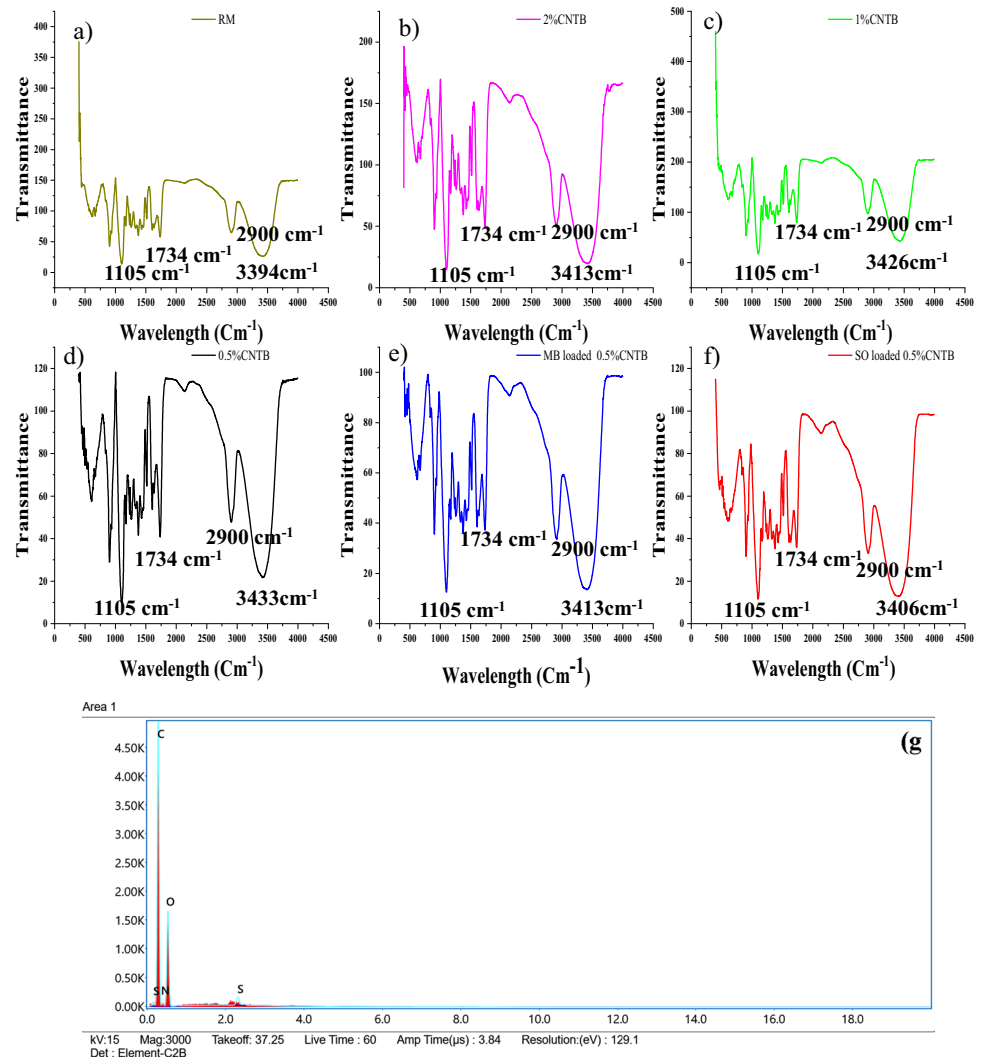
Desorption studies were performed to check the renewal efficiency of prepared adsorbents. Different eluting agents like HCl, ethanol, acetone, NaOH, and hot water were employed for the desorption of dyes. Adsorption and desorption experiments were performed up to ten cycles. In each operation, the dye-loaded adsorbents were washed in acetone to desorb the SO and MB dye adsorbed during the previous cycle. Regenerated adsorbents were oven-dried to remove moisture and stored for the later cycles.

3 Results and discussion

3.1 Physicochemical characterization of adsorbents

FTIR spectroscopy depicts different functional groups present on the surface of adsorbent which act as binding sites for MB and SO molecules. The FTIR spectrum of RM and its composites are given in Fig. 2a–d. A broad peak at 3394, 3413, 3426, and 3433 cm⁻¹ was observed in the case of RM, 2% CNTB, 1% CNTB, and 0.5% CNTB composites, respectively, ascribed to the -OH stretching. The presence of a peak at approximately 2900 cm⁻¹ was due to the methylene group C-H stretching of cellulose and hemicellulose components. The peaks around 1105 cm⁻¹ were related to C-O stretching, while the peak around 1734 cm⁻¹ was attributed to C=O [49]. After dye adsorption, the peak at 3433 cm⁻¹ in the FTIR spectrum of the 0.5% CNTB was shifted to the 3413 cm⁻¹ and 3406 cm⁻¹ in the case of MB and SO dyes, respectively, as shown in Fig. 2e–f. This shift

Fig. 2 a–d FTIR spectra of RM, 2% CNTB, 1% CNTB, and 0.5% CNTB adsorbents, e FTIR spectra of MB dye-loaded 0.5% CNTB, f FTIR spectra of SO dye-loaded 0.5% CNTB, g EDX spectra of dye-loaded 0.5% CNTB



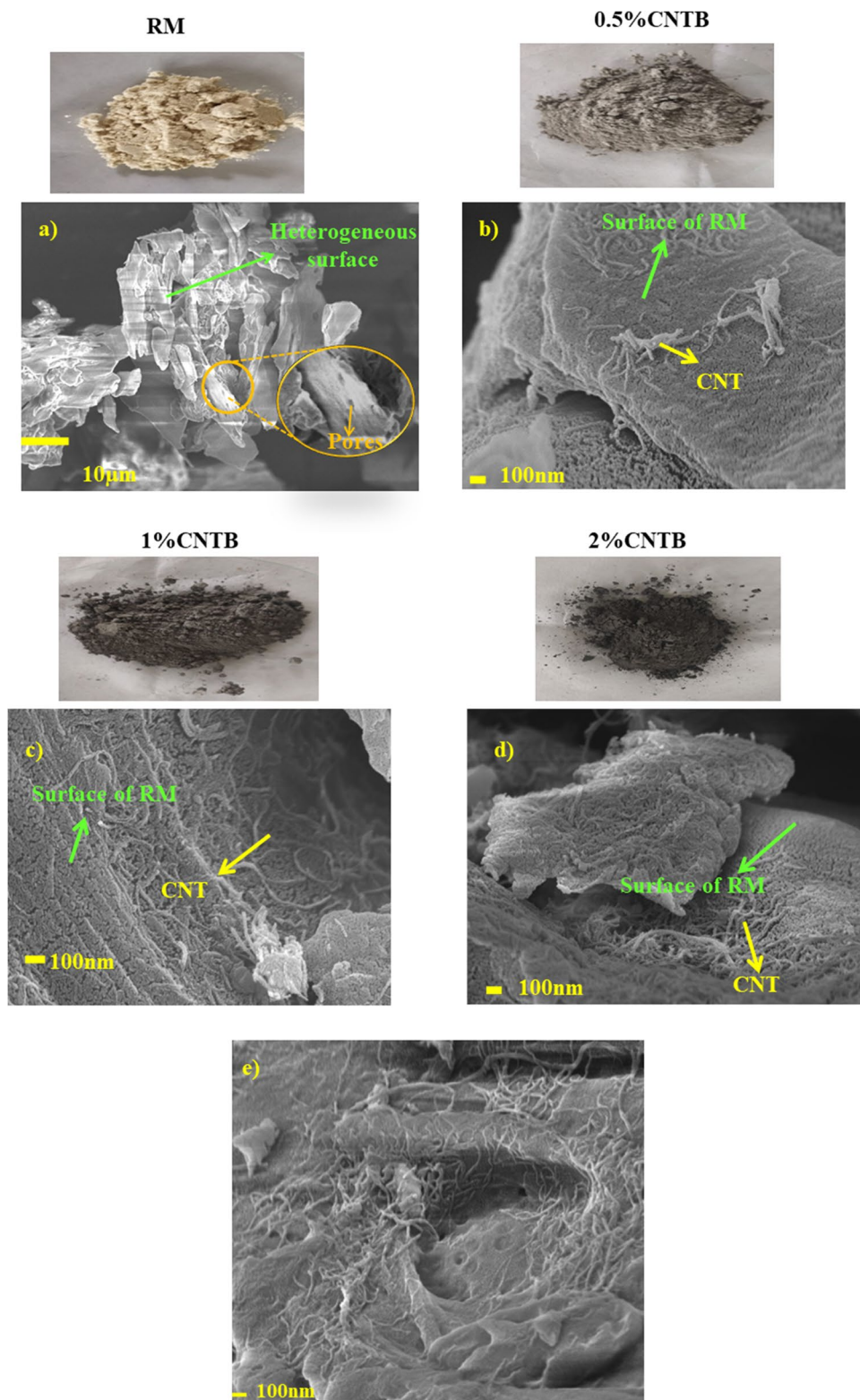
in peak indicates that the dye adsorption takes place due to hydrogen bonding between the dye molecules and the adsorbent surface. The presence of nitrogen and sulfur along with carbon and oxygen contents in the EDX spectrum of MB and SO dye-loaded adsorbent, i.e., 0.5% CNTB as depicted in Fig. 2g, shows the presence of dyes, as MB structure contains four N and one S atom, while SO contains four N atoms.

The morphologies of prepared adsorbents were investigated with the help of FESEM as shown in Fig. 3. In the FESEM image of RM, it can be seen that the adsorbent has a heterogeneous morphology involving irregular size pores, rough flakes, and sheets. After modification, the fibers of CNT on the surface of RM can be seen in FESEM images of composites. The increased roughness of surface, as well as incorporation of more functional groups due to presence of CNT, resulted in more interaction with dyes, enhancing the adsorption capacity [20] from 49.5 (MB) and 198.4 (SO) to 181.81 (MB) and 386.1 (SO) mgg^{-1} for

RM and 0.5% CNTB, respectively. After the dye adsorption, the pores on the adsorbent surface were filled with the dyes molecules as shown in Fig. 3e.

The crystalline and amorphous analysis of adsorbents was evaluated by XRD, and the obtained data of RM, 0.5% CNTB, 1% CNTB, and 2% CNTB adsorbents are given in Fig. 4a. From the analysis of adsorbent data, it was found that the strongest peak at $2\theta = 21.7^\circ$ was attributed to the cellulose crystallinity and represented the (002) crystal plane of cellulose [50]. Soldier peak at $2\theta = 15.7^\circ$ corresponded to the amorphous part of cellulose in all the adsorbents. The intense peak of CNT at $2\theta = 26.3^\circ$ appeared in 0.5% CNTB, 1% CNTB, and 2% CNTB adsorbents, and its absence in RM indicated the incorporation of functionalized CNT in raw biomass. The intensity of this peak in composite adsorbents increased by increasing the % amount of functionalized CNT. Another peak at $2\theta = 42.6^\circ$ in XRD spectra of functionalized CNT is

Fig. 3 a–d FESEM images of RM, 0.5% CNTB, 1% CNTB, and 2% CNTB adsorbents, e dye-loaded 0.5% CNTB



disappeared in composites may be attributed to the less intensity of this peak in functionalized CNT.

DSC spectra of RM, 0.5% CNTB, 1% CNTB, and 2% CNTB is given in Fig. 4b. The analysis of spectra depicts

two exothermic curves at 290 °C and 359 °C in the case of all the adsorbents but was absent in functionalized CNT. The peak at 290 °C represented the thermal degradation of hemi-cellulosic components, and the peak at 359 °C attributed to

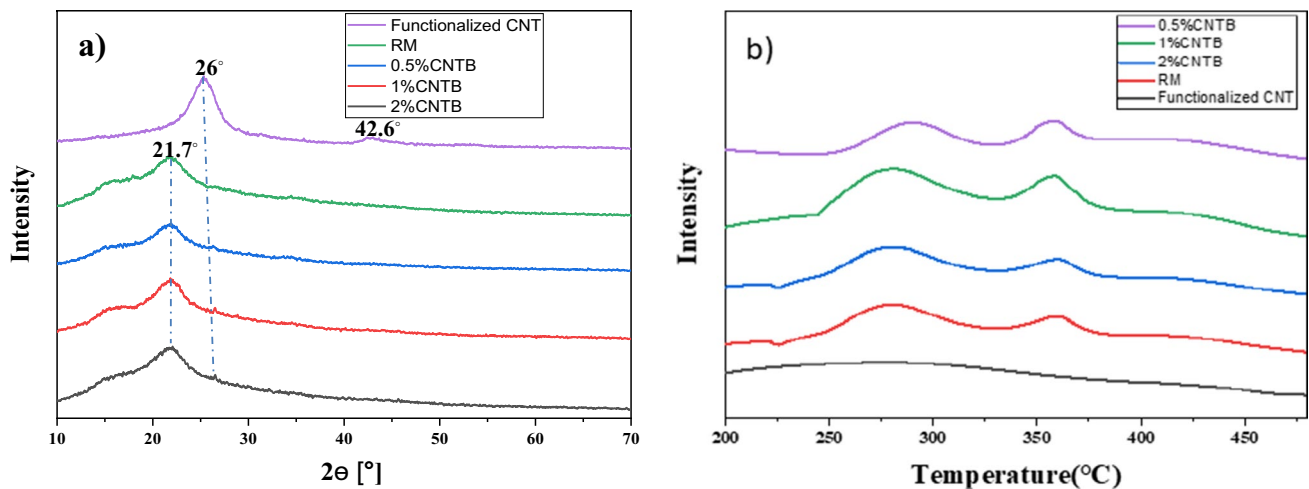


Fig. 4 a XRD spectra and b DSC spectra of functionalized CNT and RM, 0.5% CNTB, 1% CNTB, and 2% CNTB adsorbents

the decomposition of cellulose in adsorbents. In the case of functionalized CNT, there were no peaks observed up to 500 °C.

4 Batch adsorption experiments

4.1 Effect of particle size

To study the influence of particle size of RM for the removal of dyes, the 60BSS (250 μm), 80BSS (177 μm), 120BSS (125 μm), and ball milled (22.698 μm) adsorbents was taken. The dye uptake capacity and the results are shown in Fig. 5. The observed result indicated that particle size has diverse effects on the removal of dyes. The minimum % removal of 88% (SO) and 79% (MB) was observed at 250 μm and maximum % removal of 94% (SO) and 93% (MB) was found at 22.698 μm particle size. This is because of the characteristics of the nanosized adsorbent like high surface area, water holding capacity, bulk density, particle size distribution, porosity, and hydrophilicity for the adsorption of dye molecules [51]. Therefore, the ball-milled RM adsorbent was chosen for the removal of dyes molecules for further biosorption experiments.

4.2 Effect of dosage

Generally, the % removal of contaminants depends on the dosages of adsorbent. In most cases, the % removal of various contaminants increases by increasing adsorbent dosage. The effect of dosage for all the adsorbents was investigated in the range of 0.005–0.05 g in 10 mL of dye aqueous solution of concentration 30 mg L^{-1} at neutral pH and 30 °C for a contact time of 10 min to obtain the

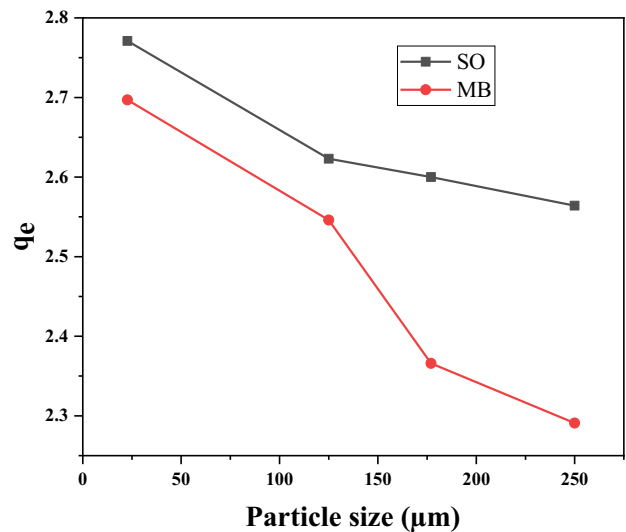


Fig. 5 Effect of particle size of RM on the adsorption of MB and SO dyes (dosage=0.01 g, dye concentration=30 mg L^{-1} , contact time=10 min, solution volume=10 mL, solution pH=7, temperature=30 °C)

optimum value of adsorbent dosage. Overall, the trend as can be seen in Fig. 6a–b was similar for all the adsorbents for the adsorption of MB and SO. By increasing dosage from 0.005 to 0.05 g in 10 mL of dye aqueous solution, the % removal was increased from 73 to 97% and 64 to 98% in the case of MB and SO dyes, respectively. The increased % removal was ascribed to the raise in contact surface area between dyes and adsorbents [52, 53]. The dosage of 0.02 g in 10 mL of dye aqueous solution was optimized for the maximum removal of dyes.

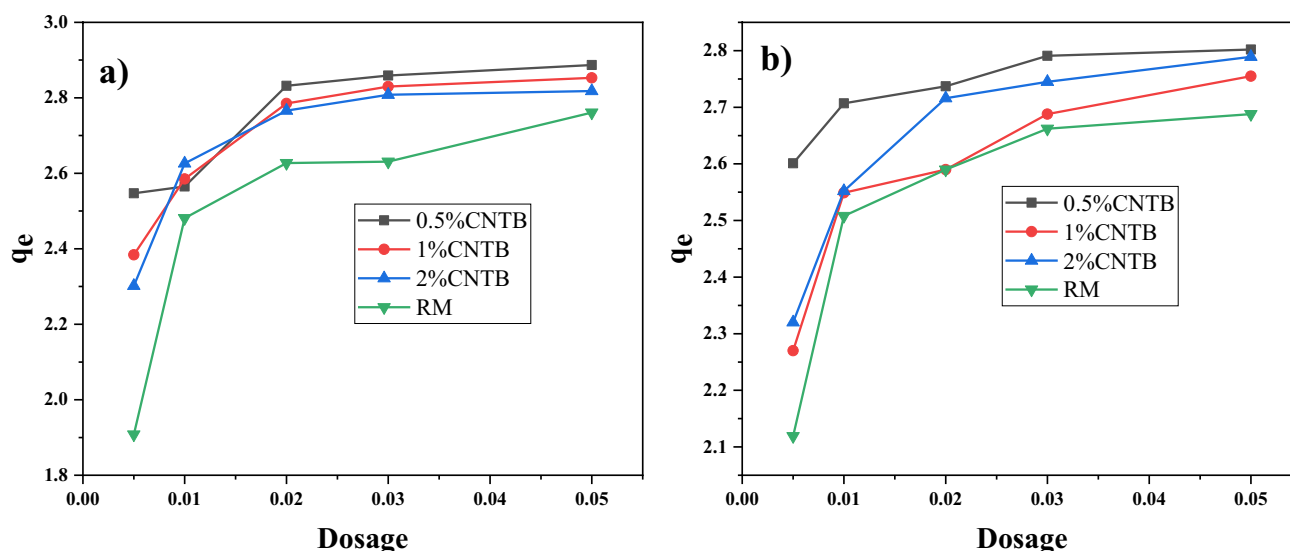


Fig. 6 Effect of adsorbent dosage on the adsorption of **a** MB and **b** SO dye (adsorbent dosage=0.005–0.05 g, dye concentration=30 mg L⁻¹, contact time=10 min, solution volume=10 mL, solution pH=7, temperature=30 °C)

4.3 Effect of pH and adsorption mechanism

The pH of the adsorption reaction system is a key factor as it influences the chemical behavior of adsorbates and the surface charge type of adsorbents [54]. pH of the solution affects the state of functional groups present on the adsorbent surface as well as measures the ionization state of adsorbate in the solution [55]. In this study, the influence of pH on the % removal for raw and composite adsorbents was investigated in the range of 2–12 at room temperature with 0.01 g in 10 mL of dye aqueous solution of dye solution for a contact time of 10 min (Fig. 7). For prepared adsorbents, the % removal was enhanced by increasing the pH value from 2 to 7 and after that, the dye removal increased slightly and remained constant. This adsorption behavior of adsorbents towards different solution pH can be explained through the relation between the dissociated state of the dye molecules and pHpzc of adsorbents. The value of pHpzc for the RM, 0.5% CNTB, 1% CNTB, and 2% CNTB adsorbents was 6.3, 6.2, 6.1, and 6.0. At pH > pHpzc, the deprotonation of surface functional groups takes place, which increased the electrostatic attraction between the negatively charged adsorbents and cationic dye molecules results in enhanced % removal [56, 57]. Therefore, pH 7.0 was optimized for further experiments. At pH < pHpzc, the surface of adsorbents was positively charged due to the protonation of carboxyl and hydroxyl functional groups, and this positive charge increased with decreasing pH. So, there was strong electrostatic repulsion between positively charged adsorbents and cationic MB and SO molecules as well as competitive effect from hydronium ions for the adsorption active sites would result in decreased removal of both dyes. But surprisingly

at acidic pH, approximately 30% removal of dyes was still observed for all the adsorbents with the existence of electrostatic repulsion between dyes and adsorbents. So, it was revealed that the electrostatic interactions were not the only interactions accountable for the adsorption process. In addition, hydrogen-bonding due to hydroxyl groups and π - π interactions could also considerably contribute to the adsorption of dyes. As the RM and its composites contain lignin and the aromatic rings in both dyes present hydrophobic properties, there was a possibility of hydrophobic-hydrophobic interactions between adsorbents and dyes.

4.4 Kinetic studies

The study of the kinetic aspect of any adsorption process is very important for pilot plant applications. Short contact time, fast reaction rate, and considerable adsorption capacity are the important conditions for an efficient adsorption process. The adsorption of MB and SO dye showed a fast dye removal up to 10 min, and after that, it becomes slow and attained equilibrium before 60 min. This adsorption behavior was attributed to the rich availability of active binding sites on the adsorbents at the initial stages with regular possession of these sites, the biosorption became constant in the later stages [58, 59]. For better elucidating the characteristics of the adsorption process such as the type of adsorption, controlling steps, saturation time, and adsorption rate, different kinetic models like pseudo-first-order, pseudo-second-order, intraparticle diffusion, and Elovich were employed [60, 61].

The calculated kinetic data were fitted best with the pseudo-second-order model (Fig. 8) in case of both the dyes, and it was confirmed by the high value of correlation

Fig. 7 Effect of pH on the adsorption of **a** SO and **b** MB by RM, 0.5% CNTB, 1% CNTB and 2% CNTB adsorbents (dosage = 0.01 g, dye concentration = 30 mg L⁻¹, contact time = 10 min, solution pH = 2–12, temperature = 30 °C)

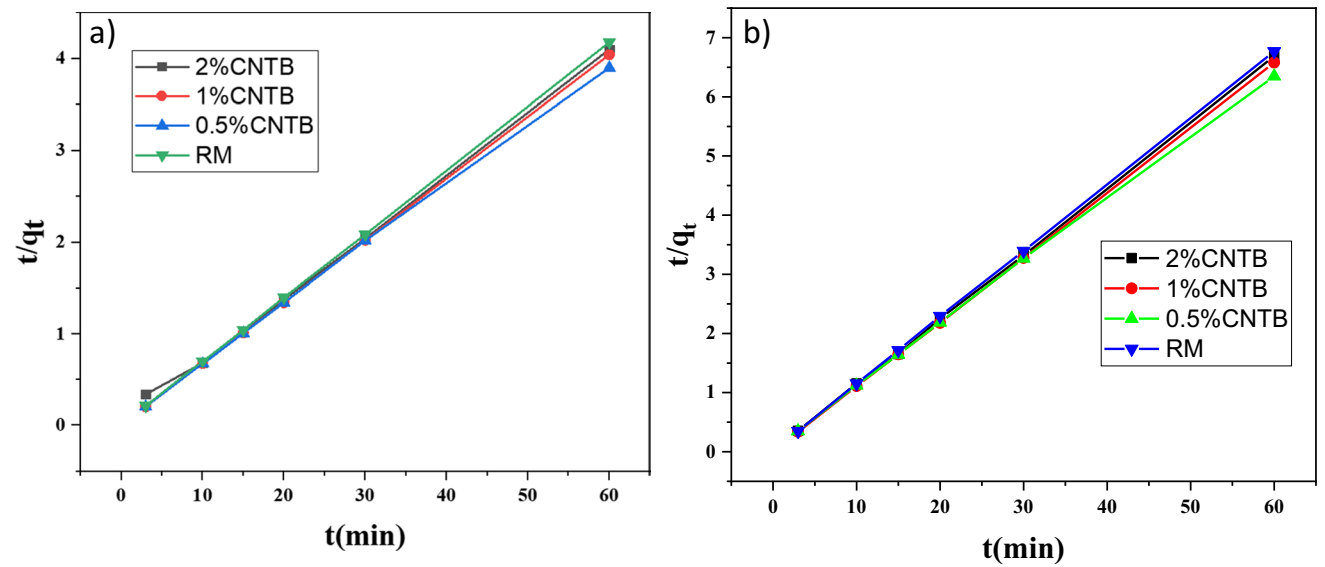
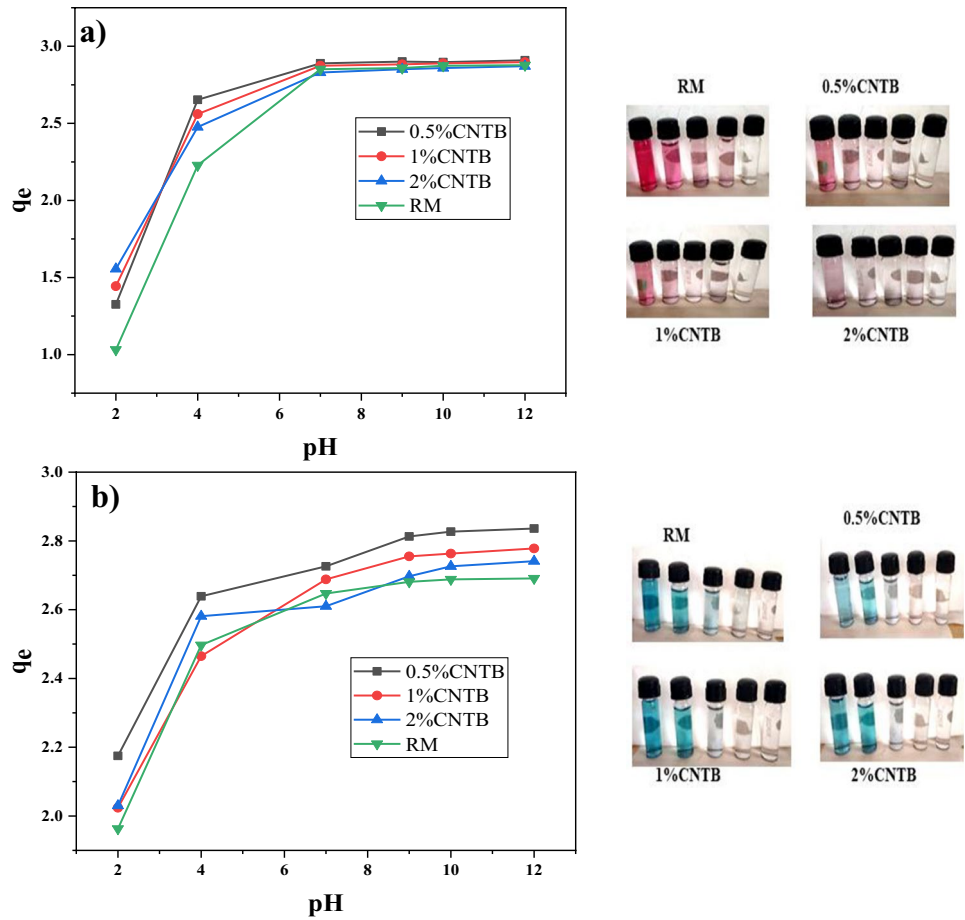


Fig. 8 Pseudo-second-order kinetic model plot of **a** SO and **b** MB (dosage = 0.01 g, dye concentration = 30 mg L⁻¹, solution volume = 10 mL, contact time = 3–60 min, solution pH = 7, temperature = 30 °C)

Table 1 Parameters of pseudo-second-order model in case of MB and SO adsorption on raw and composite adsorbents

Kinetic models	Parameters	RM		0.5%CNTB		1%CNTB		2%CNTB	
		MB	SO	MB	SO	MB	SO	MB	SO
Pseudo- second- order	$q_e(\text{mgg}^{-1})$	8.89	14.38	9.52	15.44	9.13	14.85	9.00	14.92
	$k_2(\text{min}^{-1})$	0.5	0.80	0.15	0.12	5.39	1.58	0.79	0.08
	R^2	0.99	0.99	0.99	0.99	0.99	0.99	0.99	0.99

coefficient R^2 (0.99) and proximity between $q_{e,\text{calculated}}$ and $q_{e,\text{experimental}}$ given in Table 1. This finding indicated that the chemisorption involving electrostatic action of positive and negative charges was the rate-limiting step rather than mass transfer [62, 63]. The model considers that the numbers of adsorption sites are less than adsorbate molecules. The value of pseudo-second-order rate constants was relatively higher for 1% CNTB adsorbent than others indicated the fast rate of adsorption. The q_e (mgg^{-1}) value determined from the kinetic model was (9.52 and 15.44) and from the experiment (8.9 and 14.5) for the 0.5% CNTB adsorbent in the case of MB and SO dye uptake which was higher than other adsorbents. In the case of pseudo-first-order, Elovich and intraparticle diffusion kinetic models, the value of R^2 was low as given in Table S1 and Fig. S1 (supplementary data).

4.5 Effect of dye concentration and adsorption isotherm models

The influence of concentration in the case of both dyes was investigated in the range of 15–60 mg L^{-1} . It was found that the adsorption capacity value was enhanced by increasing the initial dye concentration from 15 to 60 mg L^{-1} , but the % removal was reduced. At higher concentration, the dye ions provide a driving force to defeat the mass transfer among the solid and liquid phases, but at extremely higher concentration, the binding sites become saturated, which results in a reduction of adsorption efficiency [64]. Adsorption isotherms are useful models to describe the maximum adsorption efficiency of adsorbents, specific surface area, and pore structure of adsorbents, type of adsorption mechanism, i.e., the interaction between adsorbate and adsorbent and the equilibrium concentration of adsorbate in solution. The adsorption pattern of adsorbates such as monolayer or multilayer, chemical or physical adsorption on the adsorbent can easily be deduced from the shape of isotherm curves and appropriate results of equilibrium adsorption data [55]. The linearized expressions of isotherm models such as Langmuir, Freundlich, Dubinin-Radushkevich (D-R), and Temkin are given below [48].

$$\text{Langmuir model : } \frac{C_e}{q_e} = \frac{C_e}{q_{\max}} + \frac{1}{k_L q_{\max}} \quad (8)$$

$$\text{Freundlich model : } \ln q_e = \ln k_F + \left(\frac{1}{n}\right) \ln C_e \quad (9)$$

$$\text{Dubinin – Radushkevich model : } \ln q_e = \ln q_D - \beta \epsilon^2 \quad (10)$$

$$\text{Temkin model : } q_e = \frac{RT}{b} \ln K_t + \frac{RT}{b} \ln C_e \quad (11)$$

where q_{\max} (mgg^{-1}) represents the maximum adsorption capacity of adsorbent; q_D (mgg^{-1}) denotes the model maximum adsorption capacity; k_L (Lmg^{-1}) is the Langmuir adsorption equilibrium constant; k_F ($(\text{mg g}^{-1})(\text{L mg}^{-1})^{1/n}$) and n are the Freundlich parameters relating the adsorbed quantity and the adsorption strength, respectively; β ($\text{mol}^2 \text{kJ}^{-2}$) is a D-R model parameter, which expresses the average energy of adsorption and the mean free energy can be calculated as $E = \frac{1}{\sqrt{2\beta}}$; ϵ refers to Polay potential and its value can be calculated as $\epsilon = RT(1 + \frac{1}{C_e})$; K_t (L mol^{-1}) is the Temkin equilibrium binding constant represents the maximum binding energy; and b denotes the adsorption heat. R ($8.314 \text{ J K}^{-1} \text{ mol}^{-1}$) is the universal gas constant and T (K) is the temperature.

When the equilibrium data were fitted to the different commonly used isotherm models for the adsorption of MB and SO dye the obtained value of corresponding isotherm constants are given in Table 2, and this data fits fairly well to all the adsorption isotherms (Fig. 9). The adsorption data were best fitted with Langmuir isotherm suggesting the monolayer nature of dye adsorption at specific adsorption sites and gave the maximum adsorption capacity q_{\max} (mgg^{-1}) of value 181.81 mgg^{-1} and 386.1 mgg^{-1} for the 0.5% CNTB adsorbent in case of MB and SO dye adsorption which was higher than other adsorbents. The affinity between the adsorbate and adsorbent can be predicted by using the separation factor R_L obtained by the help of Langmuir parameters and is defined as in Eq. (12) [65].

$$R_L = \frac{1}{(1 + k_L C_0)} \quad (12)$$

R_L values indicate whether the adsorption is favorable ($0 < R_L < 1$), irreversible ($R_L = 0$), unfavourable ($R_L > 1$), and linear ($R_L = 1$). The R_L value of adsorbents was less than unity, indicating the favorability of the adsorption process. Adsorption capacity depends on the

Table 2 Isotherm parameters for the adsorption of MB and SO onto raw and composite adsorbents

Isotherms	Parameters	RM		0.5%CNTB		1%CNTB		2%CNTB	
		MB	SO	MB	SO	MB	SO	MB	SO
Langmuir	q_{max} (mgg ⁻¹)	49.5	198.4	181.81	386.1	100.9	262.0	61.3	260.4
	k_l (Lmg ⁻¹)	0.094	0.057	0.048	0.014	0.098	0.044	0.263	0.043
	R^2	0.90	0.90	0.96	0.94	0.91	0.92	0.93	0.90
Freundlich	k_f ((mgg ⁻¹) (Lmg ⁻¹) ^{1/n})	28.64	97.81	105.00	11.76	36.55	143.70	210.90	79.20
	n	1.302	0.816	1.059	0.778	1.250	0.087	1.398	0.753
	R^2	0.94	0.92	0.90	0.83	0.96	0.93	0.85	0.92
D-R	β (mole ² J ⁻²)	1.14E-7	1.01E-7	8.59E-8	3.08E-7	6.95E-8	6.43E-8	5.92E-8	1.12E-7
	E (kJmole ⁻¹)	2.97	2.20	2.41	1.30	2.68	2.80	2.91	2.10
	R^2	0.75	0.88	0.88	0.95	0.90	0.76	0.95	0.88
Temkin	K_t (Lg ⁻¹)	0.877	1.756	2.216	0.372	3.845	2.571	6.631	1.447
	$\frac{K_t}{b}$ (Jmol ⁻¹)	12.21	24.37	18.77	24.14	14.99	22.68	14.53	26.36
	R^2	0.86	0.83	0.95	0.96	0.97	0.83	0.96	0.85

value of Freundlich constant k_f ; the higher the value of k_f the more will be the adsorption efficiency. For MB adsorption, the k_f ((mg g⁻¹) (L mg⁻¹)^{1/n}) value for RM, 0.5% CNTB, 1% CNTB, and 2% CNTB was 28.64, 105, 36.55, and 210.9, respectively; in case of SO adsorption, the k_f ((mg g⁻¹) (L mg⁻¹)^{1/n}) value for RM, 0.5% CNTB, 1% CNTB, and 2% CNTB was 97.81, 11.76, 143.7, and 79.2, respectively, represented the better adsorption capacity of these adsorbents. If $1 < n < 10$, the adsorption is favorable [66]. Langmuir and Freundlich adsorption isotherms can be analyzed by using D-R and Temkin adsorption isotherms, the adsorption energy obtained by them can be employed to predict the adsorption mechanism. The values of K_t and β isotherm parameters indicated the physical nature of adsorption as the value of the free energy was less than 8 kJmol⁻¹ for all the adsorbents.

4.6 Thermodynamic study

Herein, the influence of temperature on the prepared adsorbents was investigated in the temperature range of 30–60 °C. It was recorded that the adsorption capacity was decreased from 9.016 to 8.809 mg g⁻¹ and 14.659 to 14.46 mg g⁻¹ for 0.5% CNTB composite in the case of MB and SO dye adsorption, respectively, on enhancing the temperature from 30 to 60 °C, which demonstrates the exothermic nature of the adsorption process. For all the temperatures, the change in adsorption capacity was little. So, 30 °C was taken as the optimum temperature for all the adsorption experiments. The relation between different thermodynamic parameters like Gibbs free energy (ΔG^0), entropy (ΔS^0), and enthalpy (ΔH^0) are shown in Eqs. (13–15) [67].

$$K_c = \frac{q_e}{C_e} \tag{13}$$

$$\Delta G^0 = -RT \ln K_c \tag{14}$$

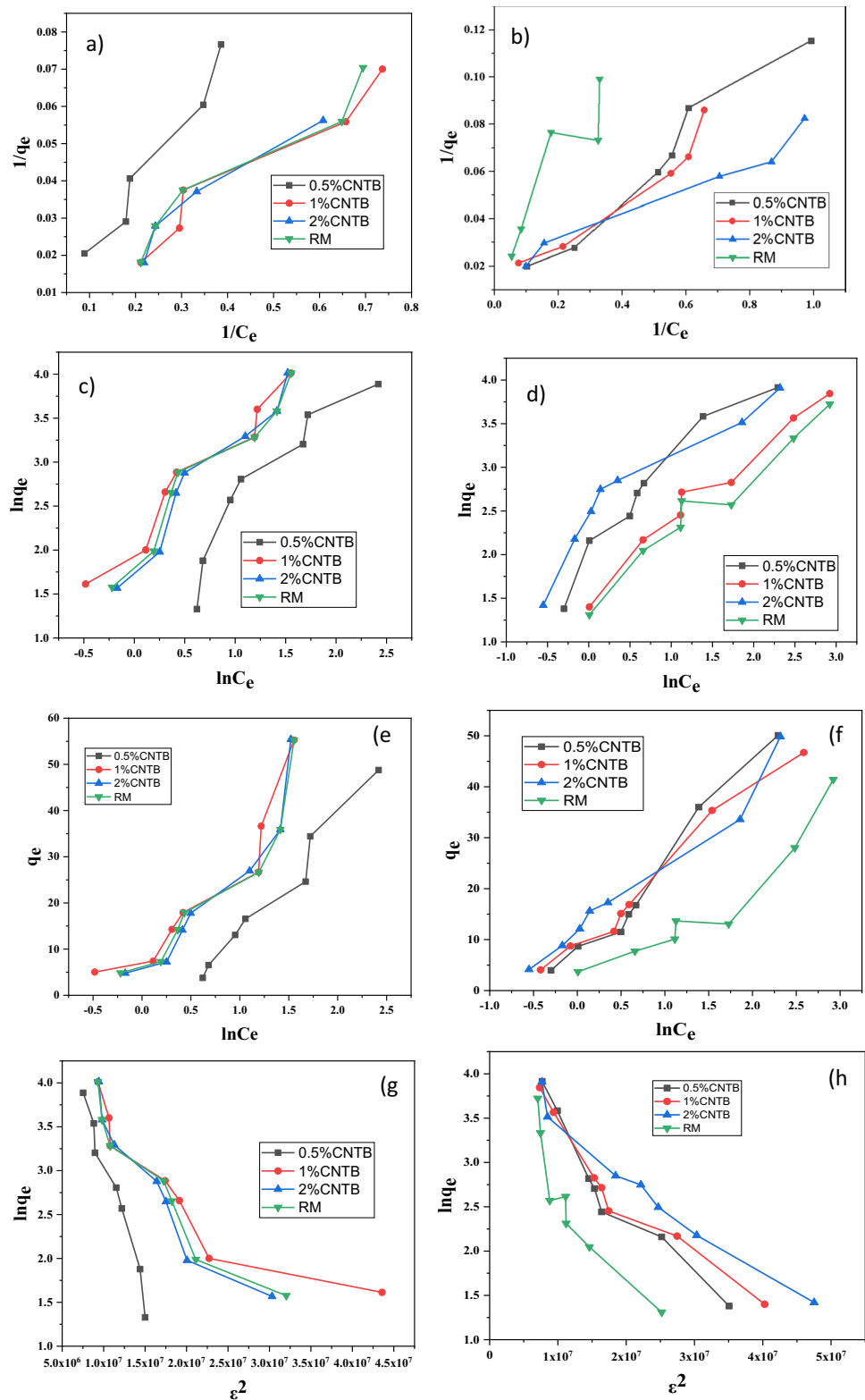
$$\ln K_c = \frac{\Delta S^0}{R} - \frac{\Delta H^0}{RT} \tag{15}$$

where K_c is the equilibrium constant and ΔH^0 and ΔS^0 values were calculated by using Arrhenius relation. Thus, the slope and intercept of the linear plot of $\ln K_c$ vs $\frac{1}{T}$ of Eq. 15 as shown in Fig. 10 gave the value of ΔH^0 and ΔS^0 . The negative values of ΔG^0 represented the spontaneous and feasible adsorption. The negative value of ΔH^0 demonstrates the exothermic nature of the adsorption process and indicated that at higher temperature the adsorption process was most likely subjected by weak interaction forces [55]. The negative value of ΔS^0 represented that during adsorption there was a reduction in the randomness at adsorbate-solution interface [68] (Table 3).

5 De-sorption and re-sorption

One of the important steps in the development of adsorption-based technologies is desorption of loaded adsorbent as the disposal of spent adsorbent to the environment is a prior concern. It enables the reuse of the biomass and recovery of the adsorbate. For the regeneration of the exhausted adsorbent, the eluent (acetone + hot water) was used. In the first cycle, the % removal by 0.5% CNTB was 98.11% and 98.81% which reduced slightly to 93.45% and 94.45% in the tenth cycle for MB and SO dyes, respectively, as represented in Fig. 11. This shows the excellent regeneration

Fig. 9 Langmuir adsorption isotherm for **a** SO and **b** MB, Freundlich adsorption isotherm for **c** SO and **d** MB, Temkin adsorption isotherm for **e** SO and **f** MB, D-R adsorption isotherm for **g** SO and **h** MB (dosage = 0.01 g, dye concentration = 15–60 mg L⁻¹, contact time = 10 min, solution volume = 10 mL, solution pH = 7, temperature = 30 °C)



ability and further reusability of adsorbents. The little but sequential reduction in % removal of dyes was ascribed to the occupation of some active sites by dye molecules after

the desorption process. The obtained results suggested that these adsorbents can be used at an industrial scale without loss in adsorption efficiency.

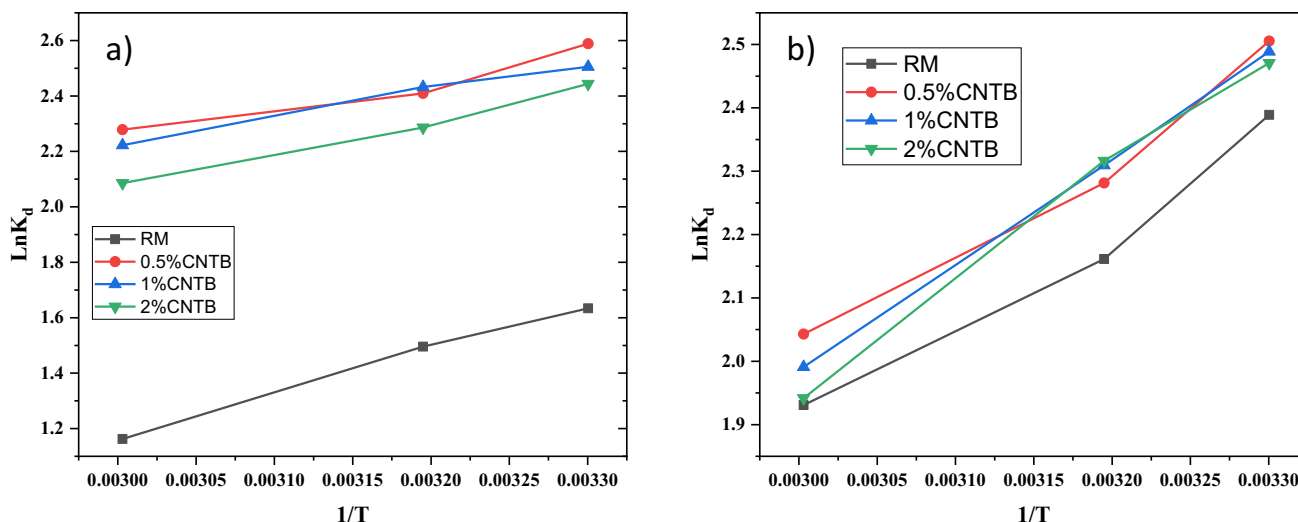
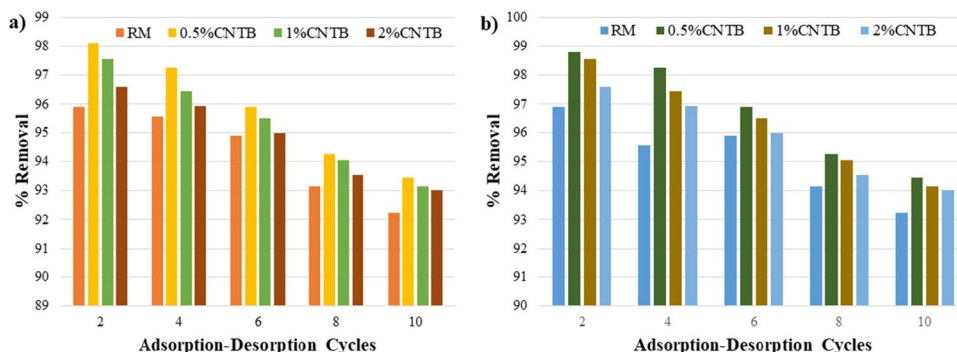


Fig. 10 Van't-Hoff plot for **a** SO adsorption and **b** MB adsorption by RM, 0.5% CNTB, 1% CNTB, and 2% CNTB adsorbents (dosage=0.01 g, dye concentration = 30 mg L⁻¹, contact time = 10 min, solution volume = 10 mL, solution pH = 7, temperature = 30–60 °C)

Table 3 Thermodynamic parameters for MB and SO dye adsorption on the raw and composite adsorbents

Adsorbents	-ΔG°(kJmol ⁻¹)			-ΔH°(kJmol ⁻¹)	-ΔS°(Jmol ⁻¹ K ⁻¹)
	303 K	313 K	333 K		
Raw(MB)	6.02	5.63	5.35	12.47	21.515
Raw(SO)	4.12	3.89	3.23	13.34	30.329
0.5%CNTB(MB)	6.31	5.94	5.66	12.62	21.016
0.5%CNTB(SO)	6.52	6.01	6.31	8.31	6.135
1%CNTB(MB)	5.02	6.02	5.52	13.91	25.207
1%CNTB(SO)	6.31	6.07	6.15	8.05	5.654
2%CNTB(MB)	6.23	6.03	5.37	14.96	28.739
2%CNTB(SO)	6.15	5.94	5.77	9.85	12.318

Fig. 11 Regeneration studies of adsorbents for removal of **a** MB dye and **b** SO dye



6 Multi-component studies

To check the adsorption efficiency of raw RM and composite adsorbents in the binary system, the experimental procedure given in the “Comparative study of biomass waste-based adsorbents for the removal of dyes” section was applied. The observed results are represented in

Fig. 12 giving that all the adsorbents have a good affinity for the SO than MB and they showed a good removal % for SO as compared to MB in binary mixture. The good affinity of SO dye may be due to the presence of four hydrogen and four nitrogen atoms which can form hydrogen bonds, π-π interactions by four benzene rings as compared to MB which involves only three benzene rings and three nitrogen atoms as shown in Fig. 13.

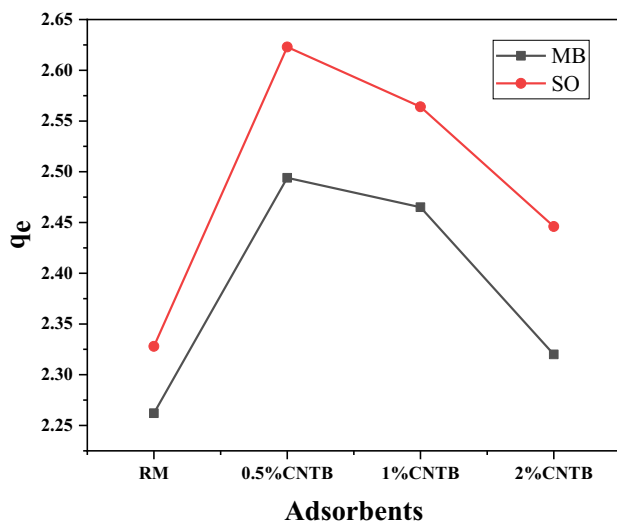


Fig. 12 % removal of MB and SO in binary mixture by RM, 0.5% CNTB, 1% CNTB, and 2% CNTB (dosage=0.01 g, dyes concentration=30 mg L⁻¹, contact time=10 min, solution volume=10 mL (5 mL SO+5 mL MB), solution pH=7, temperature=30 °C)

7 Comparative study of biomass waste-based adsorbents for the removal of dyes

Comparisons of q_{max} values obtained by the proposed adsorbents and the other biomass waste-based adsorbents reported for MB and SO dye removal are given in Table 4.

8 Conclusion and future aspects

In summary, we have successfully prepared *P. glaucum*-based CNT composites for the adsorption of MB and SO dyes from single and binary systems. To assess the

performance of the synthesized composites, % removal of dyes at different adsorbent dosages, pH, the particle size of adsorbent, initial concentration of dye, and temperature were studied. Results of the experimental adsorption data showed that the 0.5% CNTB composite exhibit very high adsorption efficiency as compared to RM and other composites with successful removal of 96 and 97% for MB and SO, respectively. The kinetic studies indicated that at the initial stage, the adsorption was rapid and equilibrium was attained below 60 min. Pseudo-second-order kinetic model was followed for MB and SO dye adsorption. From the Langmuir isotherm, the maximum adsorption capacity (q_{max}) of 0.5% CNTB adsorbent was 386.1 mg g⁻¹ for the SO adsorption and 181.81 mg g⁻¹ for the MB adsorption, respectively. From the study of thermodynamic parameters, it was observed that the adsorption process was thermodynamically feasible and exothermic. Based on the study on initial pH and FTIR analysis, the adsorption of dyes was due to hydrogen bonding, Van der Waals interactions and π - π interactions between dyes species and oxygen-containing functional groups on the surface of RM and its composite adsorbents. These adsorbents have significant dye adsorption efficiency in a binary mixture of MB and SO dye. Desorption studies indicated that all the adsorbents have a good regeneration ability up to ten cycles. The obtained results demonstrated that millet stem may be used as an effective, inexpensive, and easily used novel adsorbent for the treatment of wastewater effluents at an industrial scale. In the future, different composites of millet stem can be prepared and employed as an adsorbent for the removal of dyes, heavy metals, and emerging contaminants from wastewater effluents and with some specific modifications for the simultaneous removal of cationic and anionic dyes at neutral pH.

Fig. 13 Adsorption mechanism for removal of dyes by RM and its composites

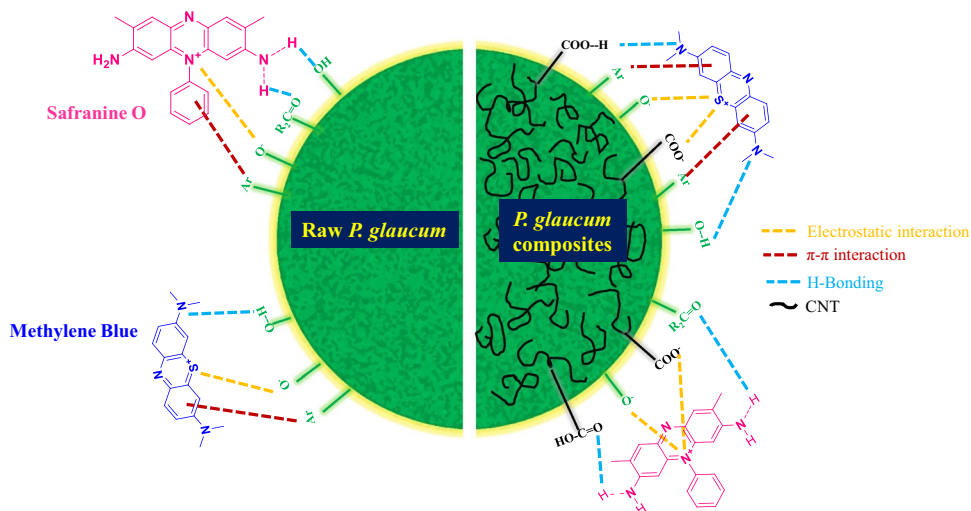


Table 4 Comparative study of biomass waste-based adsorbents for the removal of dyes

Adsorbents	Adsorbates	q _{max} (mgg ⁻¹)	References
Iron oxide/activated carbon (Sugarcane bagasse) magnetic composites	MB	36.14	[69]
<i>Palmarosa</i> (<i>Cymbopogon martinii</i>) wastes and alginate beads composite	MB	6.45	[70]
Biopolymer oak sawdust composite	MB	38.46	[71]
Magnetite nanoparticles loaded fig leaves composite	MB	61.72	[29]
Magnetite nanoparticles loaded <i>Azolla</i>	MB	25	[29]
Cellulose (banana peel waste)/SiO ₂ nanocomposite	MB	78.75	[72]
Sodium alginate and wastes of oil extraction from almond peanut composite	MB	22.8	[48]
<i>Eichhornia crassipes</i> biomass	MB	35.37	[73]
Food waste and Chinese grass residue	MB	9.5	[74]
Sugar beet pulp	SO	147	[75]
Magnetically modified <i>Sargassum horneri</i>	SO	144.4	[76]
Soybean hull	SO	29.49	[77]
Untreated coconut coir	SO	80.32	[78]
Mesoporous carbon	MB	99.15	[22]
RM	MB	49.5	Present study
0.5% CNTB	MB	181.81	Present study
1% CNTB	MB	100.9	Present study
2% CNTB	MB	61.34	Present study
RM	SO	198.4	Present study
0.5% CNTB	SO	386.1	Present study
1% CNTB	SO	262	Present study
2% CNTB	SO	260.4	Present study

Supplementary Information The online version contains supplementary material available at <https://doi.org/10.1007/s13399-021-02240-z>.

Acknowledgements The authors are thankful to CIL, Guru Jambheshwar University of Science and Technology, India for providing instrumentation facilities.

Author contribution Sarita Yadav: methodology, conceptualization, investigation, writing (reviewing and editing), original draft preparation. Aruna Yadav: writing, reviewing (editing), conceptualization. Nisha Bagotia: conceptualization, writing—reviewing and editing. Ashok K. Sharma: supervision, funding. Surender Kumar: supervision, funding, conceptualization, resources.

Funding This work was supported by Chaudhary Bansi Lal University Bhiwani, India (Grant no. CBLU/DAA/2021/1821, 2021); Haryana State Council for Science and Technology, India (Grant no. HCST/R&D/2019/1302, 2019); and University Grants Commission, India.

Declarations

Competing interests The authors declare no competing interests.

References

- Rahman Z (2020) An overview on heavy metal resistant microorganisms for simultaneous treatment of multiple chemical pollutants at co-contaminated sites, and their multipurpose application. *J. Hazard. Mater.* 396:122682. <https://doi.org/10.1016/j.jhazmat.2020.122682>
- Tan KB, Vakili M, Horri BA, Poh PE, Abdullah AZ, Salamatinia B (2015) Adsorption of dyes by nanomaterials: Recent developments and adsorption mechanisms. *Sep. Purif. Technol.* 150:229–242. <https://doi.org/10.1016/j.seppur.2015.07.009>
- Yadav A, Bagotia N, Sharma AK, Kumar S (2021) Simultaneous adsorptive removal of conventional and emerging contaminants in multi-component systems for wastewater remediation: a critical review. *Sci Total Environ* 799:149500. <https://doi.org/10.1016/j.scitotenv.2021.149500>
- Sarma GK, Khan A, El-Toni AM, Rashid MH (2019) Shape-tunable CuO-Nd(OH)₃ nanocomposites with excellent adsorption capacity in organic dye removal and regeneration of spent adsorbent to reduce secondary waste. *J Hazard Mater* 380:120838. <https://doi.org/10.1016/j.jhazmat.2019.120838>
- Li Z, Hanafy H, Zhang L, Sellaoui L, SchadeckNetto M, Oliveira MLS, Seliem MK, Luiz Dotto G, Bonilla-Petriciolet A, Li Q (2020) Adsorption of congo red and methylene blue dyes on an ashitaba waste and a walnut shell-based activated carbon from aqueous solutions: Experiments, characterization and physical interpretations. *Chem. Eng. J.* 388:124263. <https://doi.org/10.1016/j.cej.2020.124263>
- Mittal J (2020) Permissible Synthetic Food Dyes in India. *Reson. – J Sci Educ* 25:567–577
- Roy C, Dutta A, Mahapatra M, Karmakar M, Roy JSD, Mitra M, Chattopadhyay PK, Singha NR (2019) Collagenic waste and rubber based resin-cured biocomposite adsorbent for high-performance removal(s) of Hg(II), safranin, and brilliant cresyl blue: a cost-friendly waste management approach. *J Hazard Mater* 369:199–213. <https://doi.org/10.1016/j.jhazmat.2019.02.004>

8. Banerjee P, Sau S, Das P, Mukhopadhyay A (2015) Optimization and modelling of synthetic azo dye wastewater treatment using Graphene oxide nanoplatelets: Characterization toxicity evaluation and optimization using Artificial Neural Network. *Ecotoxicol Environ Saf* 119:47–57. <https://doi.org/10.1016/j.ecoenv.2015.04.022>
9. Kallel F, Chaari F, Bouaziz F, Bettaieb F, Ghorbel R, Chaabouni SE (2016) Sorption and desorption characteristics for the removal of a toxic dye, methylene blue from aqueous solution by a low cost agricultural by-product. *J Mol Liq* 219:279–288. <https://doi.org/10.1016/j.molliq.2016.03.024>
10. Liu C, Mao H, Zheng J, Zhang S (2017) Tight ultrafiltration membrane: preparation and characterization of thermally resistant carboxylated cardo poly (arylene ether ketone)s (PAEK-COOH) tight ultrafiltration membrane for dye removal. *J Memb. Sci.* 530:1–10. <https://doi.org/10.1016/j.memsci.2017.02.005>
11. Nasar A (2021) Utilization of tea wastes for the removal of toxic dyes from polluted water—a review. *Biomass Convers Biorefinery* 41–43. <https://doi.org/10.1007/s13399-020-01205-y>
12. Yadav A, Bagotia N, Sharma AK, Kumar S (2021) Advances in decontamination of wastewater using biomass-based composites: a critical review. *Sci Total Environ* 784:147108. <https://doi.org/10.1016/j.scitotenv.2021.147108>
13. Kumar N, Sinha S, Mehrotra T, Singh R, Tandon S, Thakur IS (2019) Biodecolorization of azo dye acid black 24 by *Bacillus pseudomycoloides*: process optimization using Box Behnken design model and toxicity assessment. *Bioresour. Technol. Reports* 8:100311. <https://doi.org/10.1016/j.biteb.2019.100311>
14. Bisaria K, Sinha S, Singh R, Iqbal HMN (2021) Recent advances in structural modifications of photo-catalysts for organic pollutants degradation – a comprehensive review. *Chemosphere* 284:131263. <https://doi.org/10.1016/j.chemosphere.2021.131263>
15. Mehrotra T, Zaman MN, Prasad BB, Shukla A, Aggarwal S, Singh R (2020) Rapid immobilization of viable *Bacillus pseudomycoloides* in polyvinyl alcohol/glutaraldehyde hydrogel for biological treatment of municipal wastewater. *Environ Sci Pollut Res* 27:9167–9180. <https://doi.org/10.1007/s11356-019-07296-z>
16. Chowdhury R, Mollick MMR, Biswas Y, Chattopadhyay D, Rashid MH (2018) Biogenic synthesis of shape-tunable Au-Pd alloy nanoparticles with enhanced catalytic activities. *J. Alloys Compd.* 763:399–408. <https://doi.org/10.1016/j.jallcom.2018.05.343>
17. Yang R, Li D, Li A, Yang H (2018) Adsorption properties and mechanisms of palygorskite for removal of various ionic dyes from water. *Appl. Clay Sci.* 151:20–28. <https://doi.org/10.1016/j.clay.2017.10.016>
18. Nataraj SK, Hosamani KM, Aminabhavi TM (2009) Nanofiltration and reverse osmosis thin film composite membrane module for the removal of dye and salts from the simulated mixtures. *Desalination* 249:12–17. <https://doi.org/10.1016/j.desal.2009.06.008>
19. Anastopoulos I, Pashalidis I, Orfanos AG, Manariotis ID, Tatarchuk T, Sellaoui L, Bonilla-Petriciolet A, Mittal A, Núñez-Delgado A (2020) Removal of caffeine, nicotine and amoxicillin from (waste) waters by various adsorbents. A review. *J Environ Manage* 261:110236
20. Aruna B, N., Sharma, A.K., Kumar, S., (2021) A review on modified sugarcane bagasse biosorbent for removal of dyes. *Chemosphere* 268:129309. <https://doi.org/10.1016/j.chemosphere.2020.129309>
21. Guo R, Wang R, Yin J, Jiao T, Huang H, Zhao X, Zhang L, Li Q, Zhou J, Peng Q (2019) Fabrication and highly efficient dye removal characterization of beta-cyclodextrin-based composite polymer fibers by electrospinning. *Nanomaterials.* <https://doi.org/10.3390/nano9010127>
22. Mariyam A, Mittal J, Sakina F, Baker RT, Sharma AK, Mittal A (2021) Efficient batch and Fixed-bed sequestration of a basic dye using a novel variant of ordered mesoporous carbon as adsorbent. *Arab. J. Chem.* 14:103186. <https://doi.org/10.1016/j.arabjc.2021.103186>
23. Yadav A, Bagotia N, Yadav S, Sharma AK, Kumar S (2021) Adsorptive studies on the removal of dyes from single and binary systems using saccharum munja plant-based novel functionalized CNT composites. *Environ Technol Innov* 24:102015. <https://doi.org/10.1016/j.eti.2021.102015>
24. Yadav A, Bagotia N, Yadav S, Sharma AK, Kumar S (2021d) In-situ fabrication of surfactant modified CNT-based novel bio-composite and its performance evaluation for simultaneous removal of anionic dyes: optimization by Box-Behnken design. *Sep Purif Technol* 120262. <https://doi.org/10.1016/j.seppur.2021.120262>
25. Yadav S, Yadav A, Bagotia N, Sharma AK, Kumar S (2021) Adsorptive potential of modified plant-based adsorbents for sequestration of dyes and heavy metals from wastewater - a review. *J Water Process Eng* 42:102148. <https://doi.org/10.1016/j.jwpe.2021.102148>
26. Kraus M, Trommler U, Holzer F, Kopinke F-D, Roland U (2018) Competing adsorption of toluene and water on various zeolites. *Chem. Eng. J.* 351:356–363. <https://doi.org/10.1016/j.cej.2018.06.128>
27. Siyal AA, Shamsuddin MR, Khan MI, Rabat NE, Zulfiqar M, Man Z, Siame J, Azizli KA (2018) A review on geopolymers as emerging materials for the adsorption of heavy metals and dyes. *J. Environ. Manage.* 224:327–339. <https://doi.org/10.1016/j.jenvman.2018.07.046>
28. Gupta VK, Mittal A, Jain R, Mathur M, Sikarwar S (2006) Adsorption of Safranin-T from wastewater using waste materials- activated carbon and activated rice husks. *J Colloid Interface Sci* 303:80–86. <https://doi.org/10.1016/j.jcis.2006.07.036>
29. Alizadeh N, Shariati S, Besharati N (2017) Adsorption of crystal violet and methylene blue on azolla and fig leaves modified with magnetite iron oxide nanoparticles. *Int J Environ Res* 11:197–206. <https://doi.org/10.1007/s41742-017-0019-1>
30. Mittal J, Ahmad R, Ejaz MO, Mariyam A, Mittal A (2021) A novel, eco-friendly bio-nanocomposite (Alg-Cst/Kal) for the adsorptive removal of crystal violet dye from its aqueous solutions. *Int J Phytoremediation* 1–12. <https://doi.org/10.1080/15226514.2021.1977778>
31. Abdolali A, Guo WS, Ngo HH, Chen SS, Nguyen NC, Tung KL (2014) Typical lignocellulosic wastes and by-products for biosorption process in water and wastewater treatment: a critical review. *Bioresour. Technol.* 160:57–66. <https://doi.org/10.1016/j.biortech.2013.12.037>
32. Shaikh AB, Patil DK, Kale DG, Kharad DA (2020) Analysis of variance for combining ability, gene action and heritability, proportional contribution of lines, testers and lines x testers of different characters in pearl millet (*Pennisetum glaucum* (L.). *J Pharmacogn Phytochem* 9:480–483
33. Babatunde OA, Garba S, Ali ZN (2017) Comparative adsorption capacity of modified activated carbon from *pennisetum glaucum* and sorghum bicolor. *Int J Sci Eng Res* 4
34. Batagarawa SM, Dayo LY (2017) Millet husk as efficient adsorbent for removal of lead, cadmium, and nickel ions from aqueous solution. *Dutse J. Pure Appl, Sci,* p 3
35. Charola S, Das P, Maiti S (2019) Dye adsorption using low cost carbon adsorbent from agrowaste -pearl millet cob husk. *Indian J Chem Technol* 26:35–43
36. Inbaraj S, Col RE (2002) Evaluation of a carbonaceous sorbent prepared from pearl millet husk for its removal of basic dyes. *J Sci Ind Res (India)* 61:971–978

37. Selvapandian P, Ananthakumar K, Cyril A (2015) Biosorption of crystal violet from aqueous solution by pearl millet powder : Isotherm modelling and kinetic studies. *J Appl Res water wastewater* 4:143–149
38. Yousaf A, Athar M, Salman M, Farooq U (2017) Biosorption characteristics of *Pennisetum glaucum* for the removal of Pb(II), Ni(II) and Cd(II) ions from aqueous medium. *Green Chem Lett Rev* 10:462–470. <https://doi.org/10.1080/17518253.2017.1402093>
39. Tian Y, Gao B, Morales VL, Wu L, Wang Y, Muñoz-Carpena R, Cao C, Huang Q, Yang L (2012) Methods of using carbon nanotubes as filter media to remove aqueous heavy metals. *Chem. Eng. J.* 210:557–563. <https://doi.org/10.1016/j.cej.2012.09.015>
40. Zhang J, Huang Z-H, Lv R, Yang Q-H, Kang F (2009) Effect of growing CNTs onto bamboo charcoals on adsorption of copper ions in aqueous solution. *Langmuir* 25:269–274. <https://doi.org/10.1021/la802365w>
41. Ma J, Yu F, Zhou L, Jin L, Yang M, Luan J, Tang Y, Fan H, Yuan Z, Chen J (2012) Enhanced adsorptive removal of methyl orange and methylene blue from aqueous solution by alkali-activated multiwalled carbon nanotubes. *ACS Appl Mater Interfaces* 4:5749–5760. <https://doi.org/10.1021/am301053m>
42. Theodore M, Hosur M, Thomas J, Jeelani S (2011) Influence of functionalization on properties of MWCNT–epoxy nanocomposites. *Mater. Sci. Eng. A* 528:1192–1200. <https://doi.org/10.1016/j.msea.2010.09.095>
43. Wang S (2009) Optimum degree of functionalization for carbon nanotubes. *Curr. Appl. Phys.* 9:1146–1150. <https://doi.org/10.1016/j.cap.2009.01.004>
44. Inyang M, Gao B, Zimmerman A, Zhang M, Chen H (2014) Synthesis, characterization, and dye sorption ability of carbon nanotube-biochar nanocomposites. *Chem Eng J* 236:39–46. <https://doi.org/10.1016/j.cej.2013.09.074>
45. Gupta VK, Kumar R, Nayak A, Saleh TA, Barakat MA (2013) Adsorptive removal of dyes from aqueous solution onto carbon nanotubes: a review. *Adv Colloid Interface Sci* 193–194:24–34. <https://doi.org/10.1016/j.cis.2013.03.003>
46. Saharan P, Sharma AK, Kumar V, Kaushal I (2019) Multifunctional CNT supported metal doped MnO₂ composite for adsorptive removal of anionic dye and thiourea sensing. *Mater. Chem. Phys.* 221:239–249. <https://doi.org/10.1016/j.matchemphys.2018.09.001>
47. Yang Y, Chun Y, Shang G, Huang M (2004) pH-dependence of pesticide adsorption by wheat-residue-derived black carbon. *Langmuir* 20:6736–6741. <https://doi.org/10.1021/la049363t>
48. Erfani M, Javanbakht V (2018) Methylene Blue removal from aqueous solution by a biocomposite synthesized from sodium alginate and wastes of oil extraction from almond peanut. *Int J Biol Macromol* 114:244–255. <https://doi.org/10.1016/j.ijbiomac.2018.03.003>
49. Xing Y, Deng D (2009) Enhanced adsorption of malachite green by EDTAD-modified sugarcane bagasse. *Sep. Sci. Technol.* 44:2117–2131. <https://doi.org/10.1080/01496390902775588>
50. Wang T, Li C, Wang C, Wang H (2018) Biochar/MnAl-LDH composites for Cu (II) removal from aqueous solution. *Colloids Surfaces A Physicochem Eng Asp* 538:443–450. <https://doi.org/10.1016/j.colsurfa.2017.11.034>
51. Bisht D, Sinha S, Nigam S, Bisaria K, Mehrotra T, Singh R (2021) Adsorptive decontamination of paper mill effluent by nano fly ash: response surface methodology, adsorption isotherm and reusability studies. *Water Sci. Technol.* 83:1662–1676. <https://doi.org/10.2166/wst.2021.066>
52. Mushtaq M, Bhatti HN, Iqbal M, Noreen S (2016) Eriobotrya japonica seed biocomposite efficiency for copper adsorption: Isotherms, kinetics, thermodynamic and desorption studies. *J Environ Manage* 176:21–33. <https://doi.org/10.1016/j.jenvman.2016.03.013>
53. Ullah I, Nadeem R, Iqbal M, Manzoor Q (2013) Biosorption of chromium onto native and immobilized sugarcane bagasse waste biomass. *Ecol. Eng.* 60:99–107. <https://doi.org/10.1016/j.ecoleng.2013.07.028>
54. Yagub MT, Sen TK, Afroze S, Ang HM (2014) Dye and its removal from aqueous solution by adsorption : A review. *Adv Colloid Interface Sci* 209:172–184. <https://doi.org/10.1016/j.cis.2014.04.002>
55. Chen B, Long F, Chen S, Cao Y, Pan X (2020) Magnetic chitosan biopolymer as a versatile adsorbent for simultaneous and synergistic removal of different sorts of dyestuffs from simulated wastewater. *Chem. Eng. J.* 385:123926. <https://doi.org/10.1016/j.cej.2019.123926>
56. Salazar-Rabago JJ, Leyva-Ramos R, Rivera-Utrilla J, Ocampo-Perez R, Cerino-Cordova FJ (2017) Biosorption mechanism of Methylene Blue from aqueous solution onto White Pine (*Pinus durangensis*) sawdust: Effect of operating conditions. *Sustain. Environ. Res.* 27:32–40. <https://doi.org/10.1016/j.serj.2016.11.009>
57. Tang Y, Lin T, Jiang C, Zhao Y, Ai S (2021) Renewable adsorbents from carboxylate-modified agro-forestry residues for efficient removal of methylene blue dye. *J Phys Chem Solids* 149:109811. <https://doi.org/10.1016/j.jpcs.2020.109811>
58. Pillai SS, Mullassery MD, Fernandez NB, Giriya N, Geetha P, Koshy M (2013) Biosorption of Cr(VI) from aqueous solution by chemically modified potato starch: equilibrium and kinetic studies. *Ecotoxicol. Environ. Saf.* 92:199–205. <https://doi.org/10.1016/j.ecoenv.2013.01.020>
59. Yahaya YA, Mat Don M, Bhatia S (2009) Biosorption of copper (II) onto immobilized cells of *Pycnoporus sanguineus* from aqueous solution: equilibrium and kinetic studies. *J. Hazard. Mater.* 161:189–195. <https://doi.org/10.1016/j.jhazmat.2008.03.104>
60. Ahmed MJ (2017) Adsorption of quinolone, tetracycline, and penicillin antibiotics from aqueous solution using activated carbons: review. *Environ. Toxicol. Pharmacol.* 50:1–10. <https://doi.org/10.1016/j.etap.2017.01.004>
61. Tan KL, Hameed BH (2017) Insight into the adsorption kinetics models for the removal of contaminants from aqueous solutions. *J. Taiwan Inst. Chem. Eng.* 74:25–48. <https://doi.org/10.1016/j.jtice.2017.01.024>
62. Chen S, Zhou M, Wang HF, Wang T, Wang XS, Hou HB, Song BY (2018) Adsorption of reactive brilliant Red X-3B in aqueous solutions on clay-biochar composites from bagasse and natural attapulgite. *Water* 10:703. <https://doi.org/10.3390/w10060703>
63. Isaac PJ, Amaravadi S, M.S.M., K., Cheralathan, K.K., Lakshmi pathy, R., (2019) Synthesis of zeolite/activated carbon composite material for the removal of lead (II) and cadmium (II) ions. *Environ Prog Sustain Energy* 38:133–140. <https://doi.org/10.1002/ep.13246>
64. Bhatti HN, Jabeen A, Iqbal M, Noreen S, Naseem Z (2017) Adsorptive behavior of rice bran-based composites for malachite green dye: isotherm, kinetic and thermodynamic studies. *J. Mol. Liq.* 237:322–333. <https://doi.org/10.1016/j.molliq.2017.04.033>
65. Peng S-H, Wang R, Yang L-Z, He L, He X, Liu X (2018) Biosorption of copper, zinc, cadmium and chromium ions from aqueous solution by natural foxtail millet shell. *Ecotoxicol. Environ. Saf.* 165:61–69. <https://doi.org/10.1016/j.ecoenv.2018.08.084>
66. Abedi S, Zavvar Mousavi H, Asghari A (2016) Investigation of heavy metal ions adsorption by magnetically modified aloe vera leaves ash based on equilibrium, kinetic and thermodynamic studies. *Desalin Water Treat* 57:13747–13759. <https://doi.org/10.1080/19443994.2015.1060536>
67. Edathil AA, Shittu I, Hisham Zain J, Banat F, Haija MA (2018) Novel magnetic coffee waste nanocomposite as effective

- bioadsorbent for Pb(II) removal from aqueous solutions. *J Environ Chem Eng* 6:2390–2400. <https://doi.org/10.1016/j.jece.2018.03.041>
68. Lafi R, Montasser I, Hafiane A (2019) Adsorption of congo red dye from aqueous solutions by prepared activated carbon with oxygen-containing functional groups and its regeneration. *Adsorpt Sci Technol* 37:160–181. <https://doi.org/10.1177/0263617418819227>
69. Jiang W, Zhang L, Guo X, Yang M, Lu Y, Wang Y, Zheng Y, Wei G (2021) Adsorption of cationic dye from water using an iron oxide/activated carbon magnetic composites prepared from sugarcane bagasse by microwave method. *Environ Technol* 42:337–350. <https://doi.org/10.1080/09593330.2019.1627425>
70. Saha A, Tripathy V, Basak BB, Kumar J (2018) Entrapment of distilled palmarosa (*cymbopogon martinii*) wastes in alginate beads for adsorptive removal of methylene blue from aqueous solution. *Environ Prog Sustain Energy* 37:1942–1953. <https://doi.org/10.1002/ep.12872>
71. El-Latif MMA, Ibrahim AM, El-Kady MF (2010) Adsorption equilibrium, kinetics and thermodynamics of methylene blue from aqueous solutions using biopolymer oak sawdust composite. *J Am Sci* 6:267–283
72. Ali SM (2018) Fabrication of a nanocomposite from an agricultural waste and its application as a biosorbent for organic pollutants. *Int J Environ Sci Technol* 15:1169–1178. <https://doi.org/10.1007/s13762-017-1477-x>
73. Viswanthan SP, Neelamury SP, Parakkuzhiyil S, Njzhakunnathu GV, Sebastian A, Padmakumar B, Ambatt TP (2020) Removal efficiency of methylene blue from aqueous medium using biochar derived from *Phragmites karka*, a highly invasive wetland weed. *Biomass Convers Biorefinery* 1–17. <https://doi.org/10.1007/s13399-020-00877-w>
74. Fazal T, Faisal A, Mushtaq A, Hafeez A, Javed F, Alaud Din A, Rashid N, Aslam M, Rehman MSU, Rehman F (2019) Macroalgae and coal-based biochar as a sustainable bioresource reuse for treatment of textile wastewater. *Biomass Convers. Biorefinery* 11:1491–1506. <https://doi.org/10.1007/s13399-019-00555-6>
75. Malekbala Mohamad Rasool, Hosseini S, KazemiYazdi S, MasoudiSoltani S, Malekbala Mohammad Rahim (2012) The study of the potential capability of sugar beet pulp on the removal efficiency of two cationic dyes. *Chem. Eng. Res. Des.* 90:704–712. <https://doi.org/10.1016/j.cherd.2011.09.010>
76. Angelova R, Baldikova E, Pospiskova K, Maderova Z, Safarikova M, Safarik I (2016) Magnetically modified *Sargassum horneri* biomass as an adsorbent for organic dye removal. *J. Clean. Prod.* 137:189–194. <https://doi.org/10.1016/j.jclepro.2016.07.068>
77. Chandane V, Singh VK (2016) Adsorption of safranin dye from aqueous solutions using a low-cost agro-waste material soybean hull. *Desalin. Water Treat.* 57:4122–4134. <https://doi.org/10.1080/19443994.2014.991758>
78. Ghosh I, Kar S, Chatterjee T, Bar N, Das SK (2021) Adsorptive removal of safranin-O dye from aqueous medium using coconut coir and its acid-treated forms: adsorption study, scale-up design, MPR and GA-ANN modeling. *Sustain Chem Pharm* 19:100374. <https://doi.org/10.1016/j.scp.2021.100374>

Publisher's Note Springer Nature remains neutral with regard to jurisdictional claims in published maps and institutional affiliations.